Simplifying the Dynamics of the Atlantic Meridional Overturning Circulation at 26°N

Emma Worthington

Gerard McCarthy, Robert Marsh, Jenny Mecking, Sybren Drijfhout

PhD confirmation presentation, 27 June 2019

Overview

- Atlantic Meridional Overturning Circulation
- Why do we want to simplify its dynamics?
- Multiple linear regression models
- Conclusions

Atlantic Meridional Overturning Circulation

(AMOC)

AMOC observed by RAPID array at 26°N

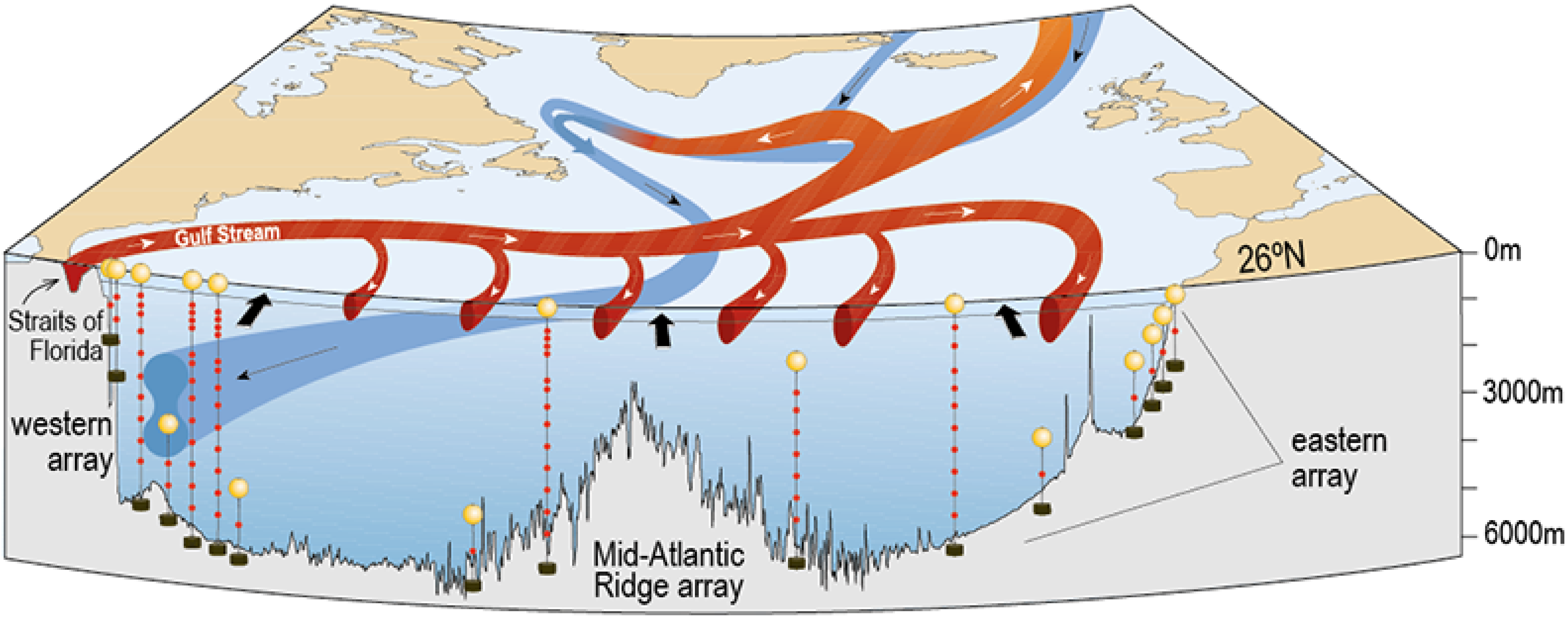

[www.rapid.ac.uk]

Observations of the AMOC

Hydrographic sections

1957 to 2004

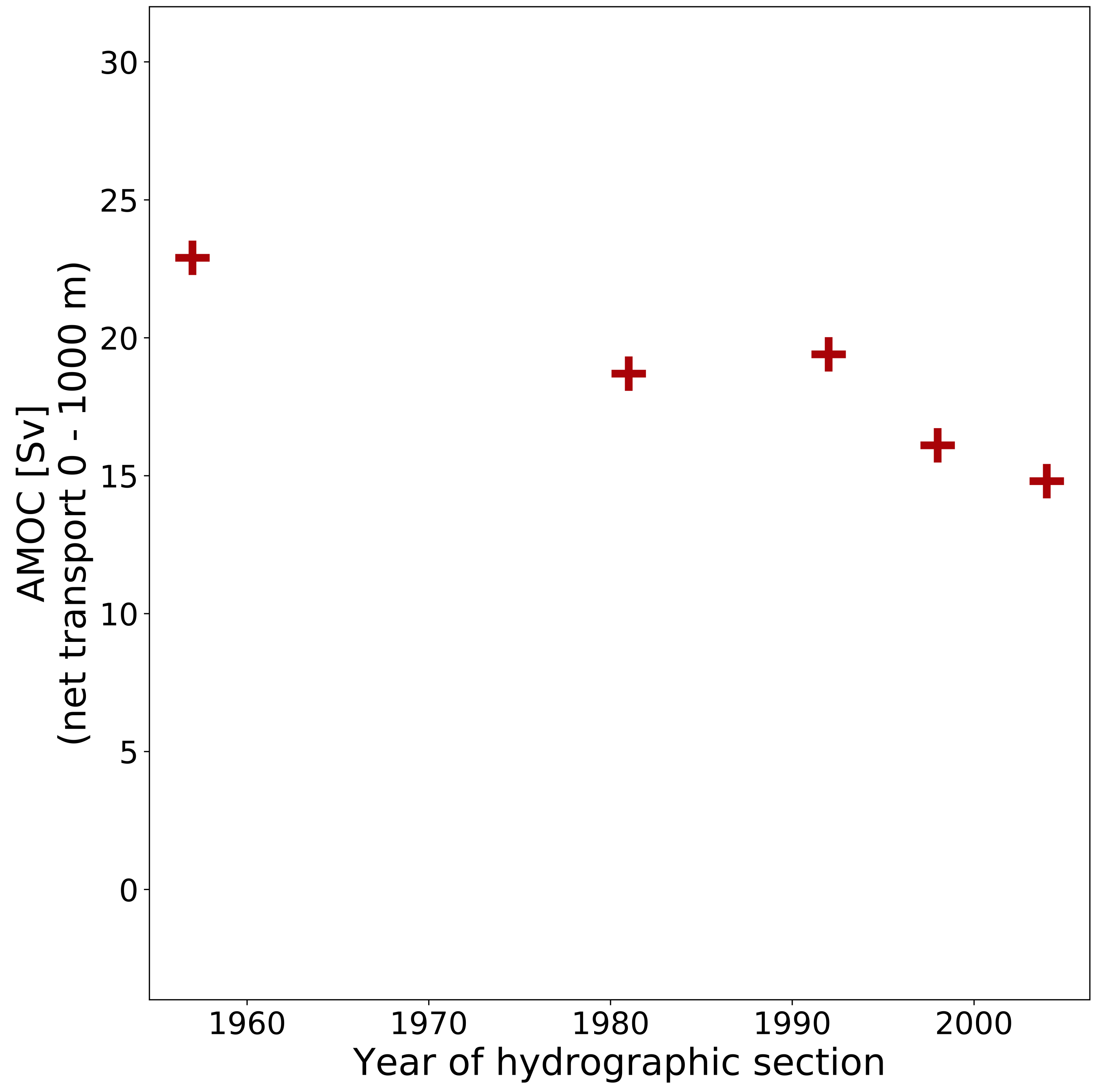

[Data from Bryden et al., (2005)]

RAPID timeseries

2004 to present

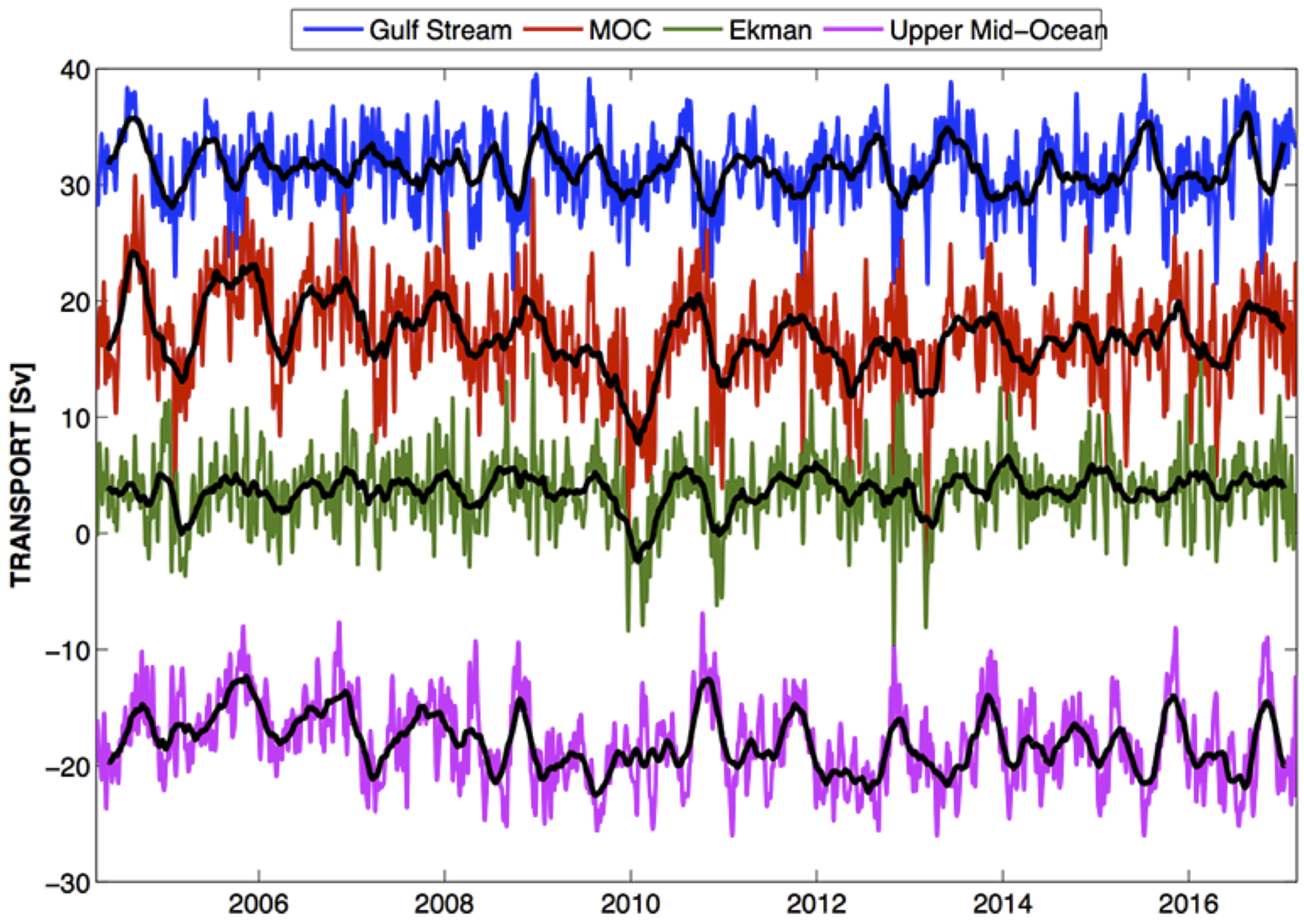

[www.rapid.ac.uk]

Can we learn more about the AMOC before 2004?

- Other hydrographic data is available prior to 2004
  - e.g. repeat CTDs, short mooring arrays
  - not sufficient to estimate AMOC as RAPID does
- Proxy for thermocline transport — temperature at a depth of 400 dbar at the western boundary (WB) *[Longworth et al. (2011)]*

39 values between 1986 and 1998

Repeat WB CTD stations

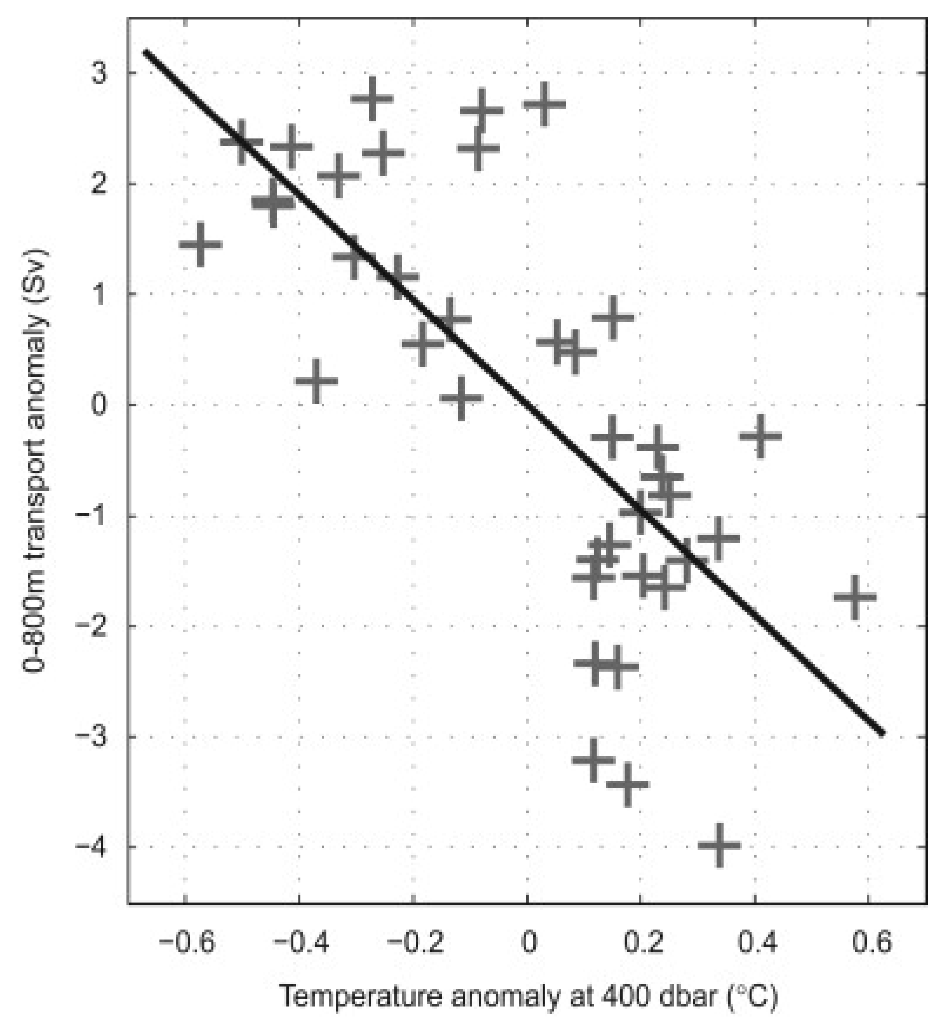

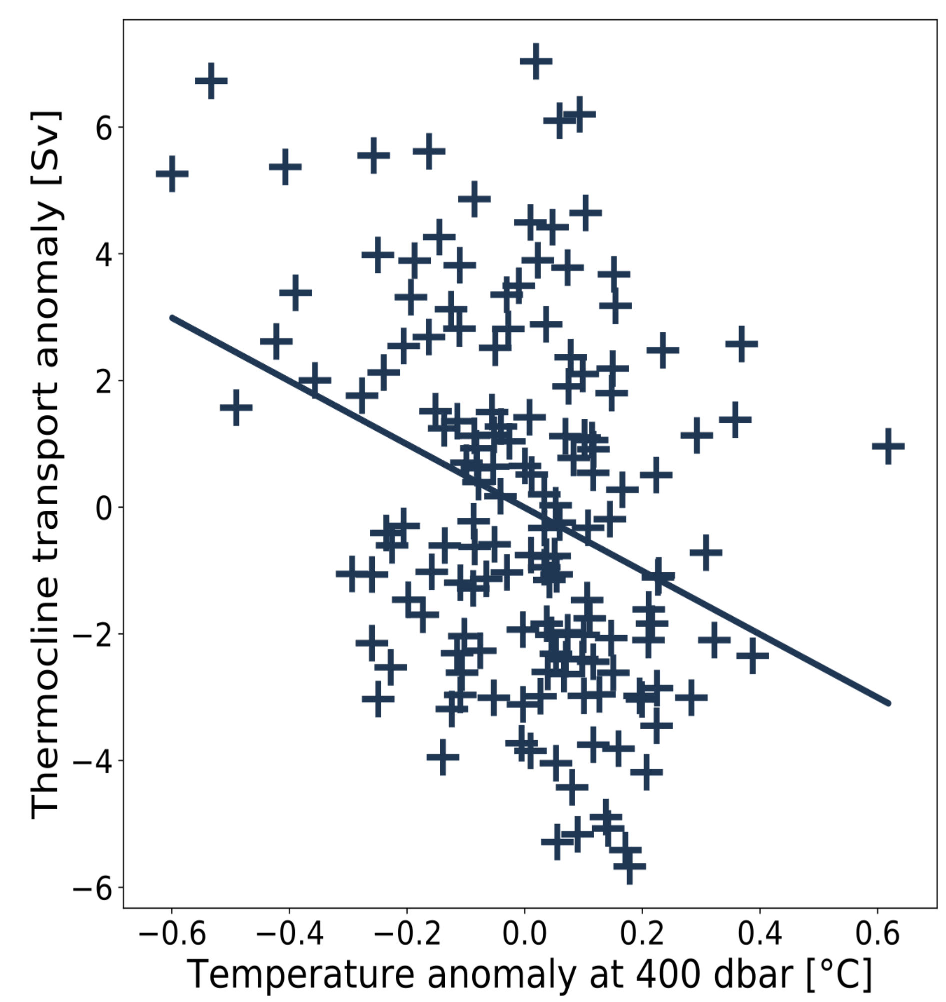

155 monthly mean values between 2004 and 2017

RAPID WB profile

Longworth regression model explained 53% of the observed thermocline transport variance

RAPID data regression model explains only 10%

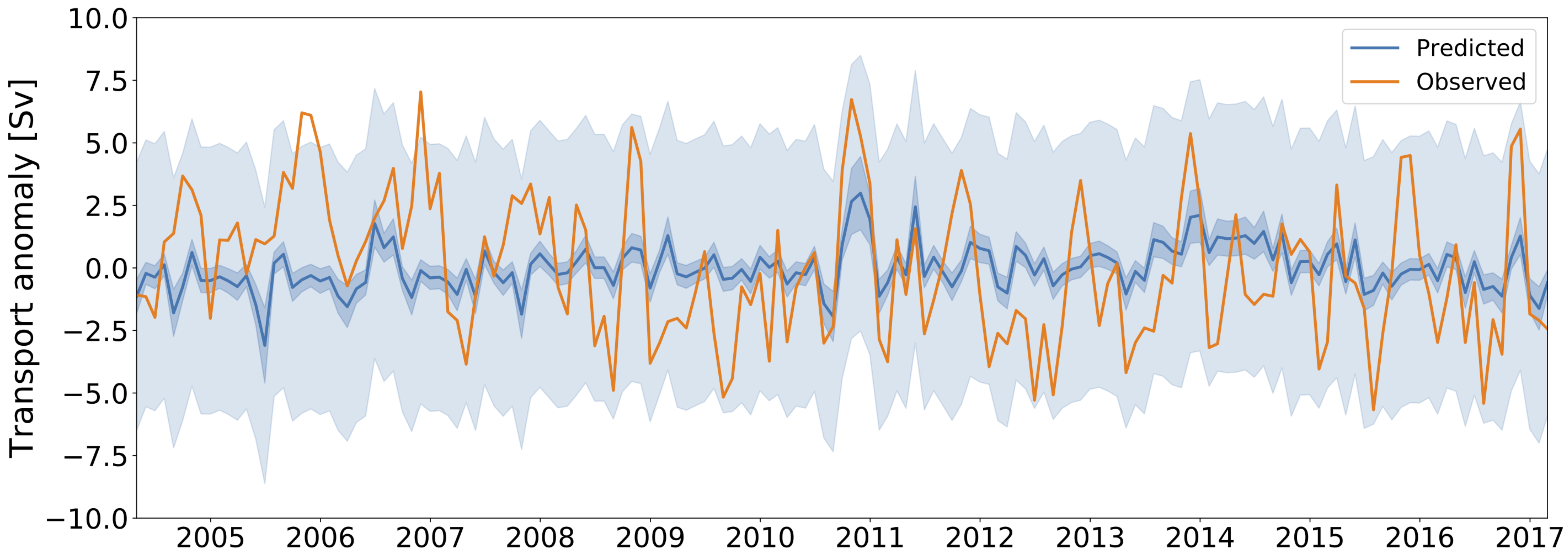

How can it be improved?

Using the temperature anomaly at 780 dbar depth improves explained variance to 33%

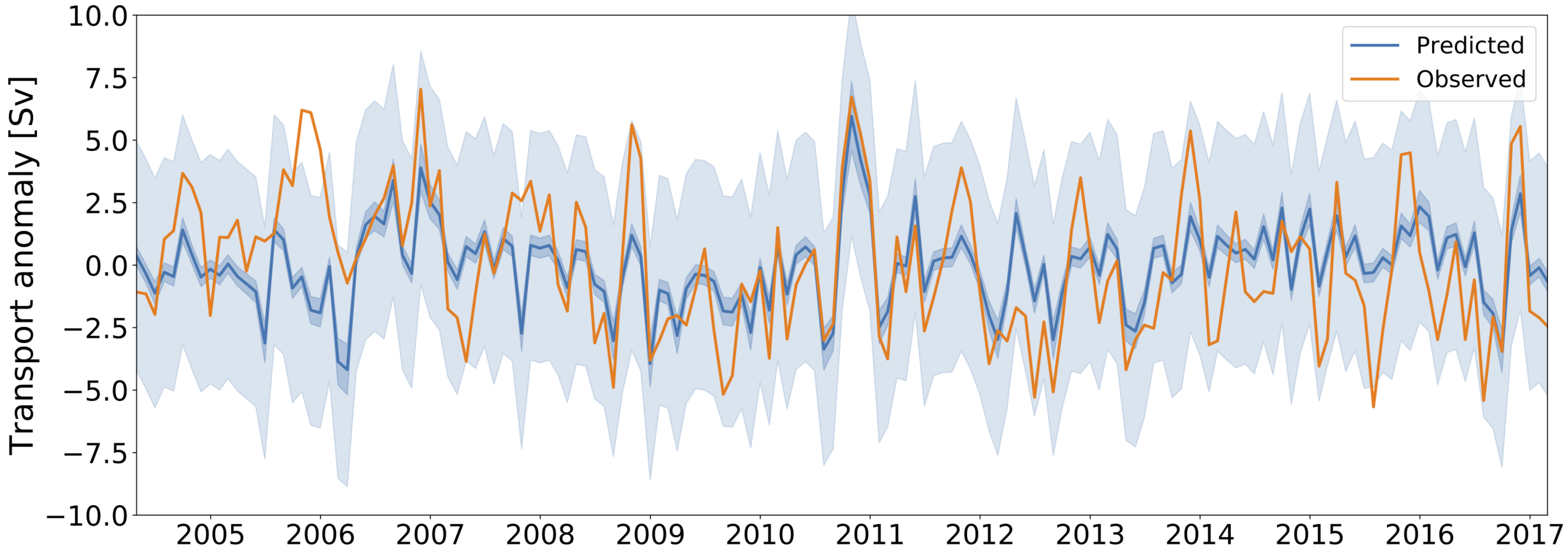

What does the mid-ocean overturning circulation look like at 26°N?

Density

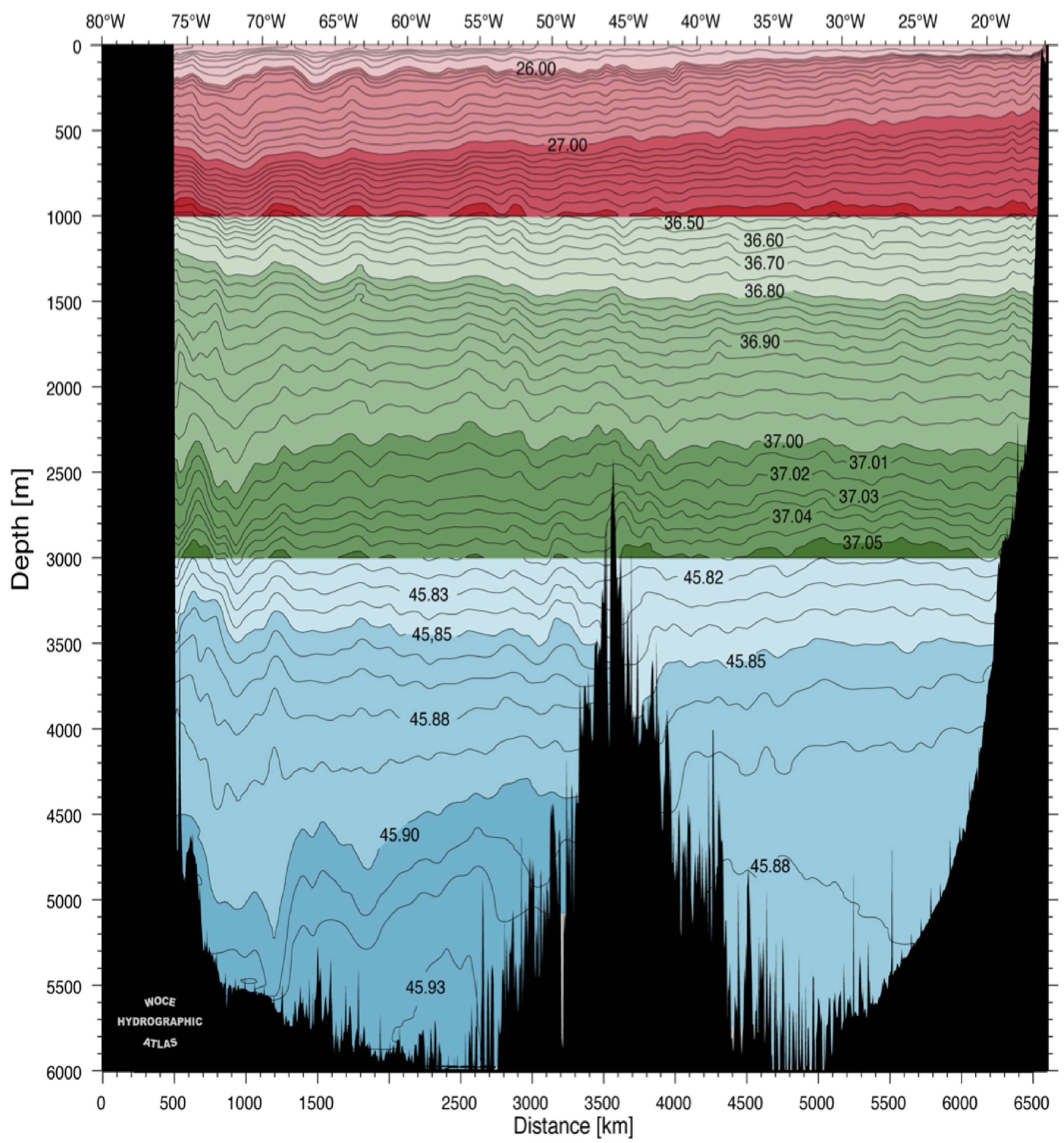

$$\frac{\partial \rho}{\partial x} = -\frac{f\rho_0}{g}\frac{\partial v}{\partial z}$$

EB > WB = negative shear

WB > EB = positive shear

Isopycnals slope up to the east above 1000 m, down to the east below

Mid-ocean transport

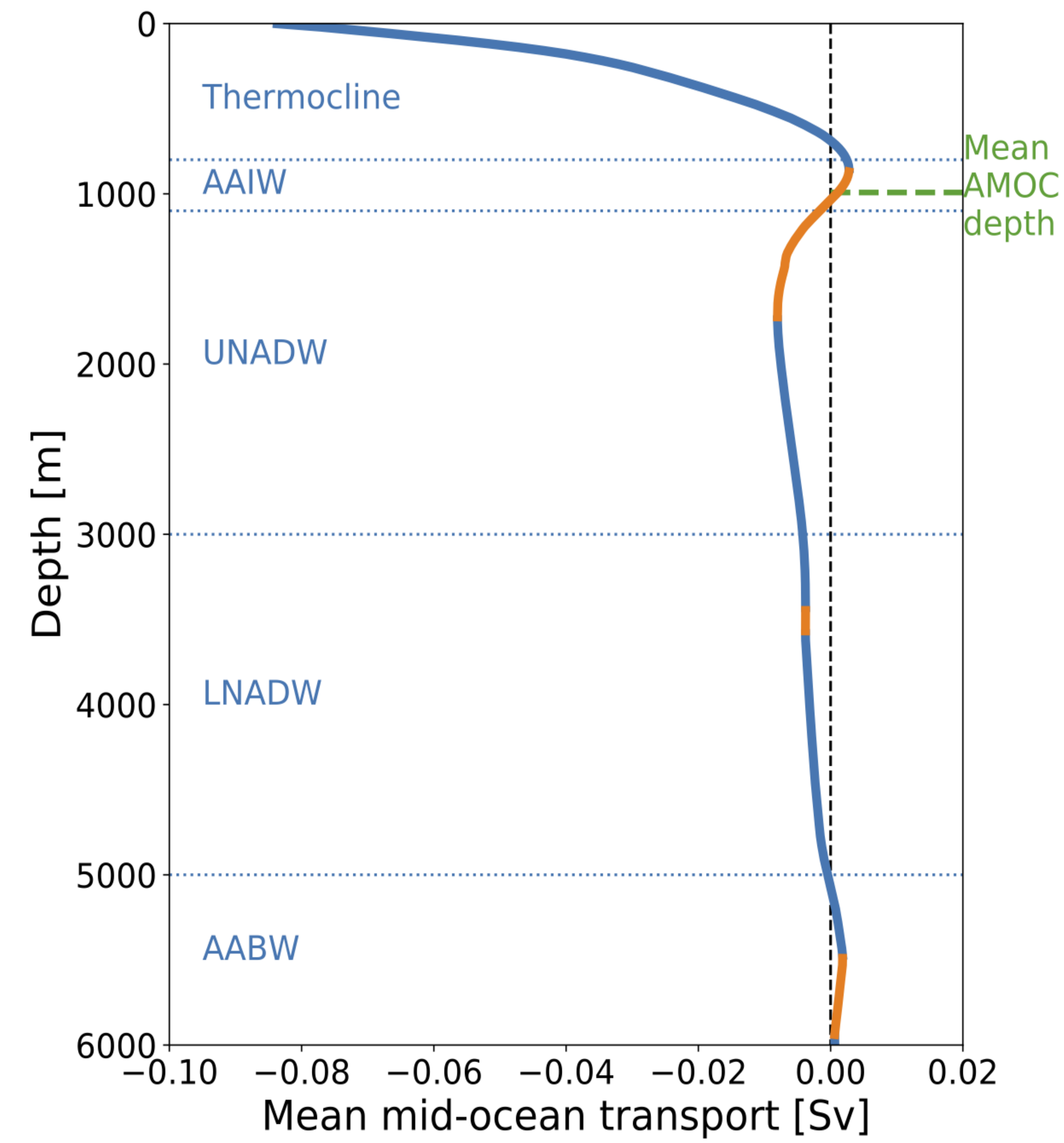

Southwards above ~800 m and below ~1100 m, with an intermediate northwards layer

Variability in the mid-ocean (geostrophic) AMOC component is defined by partition between two southwards transports:

Recirculation in the upper layer	vs.	Deep overturning return flow (NADW)

To capture this variability, at least 3 layers need to be represented by the regression model

Changes in layer thickness

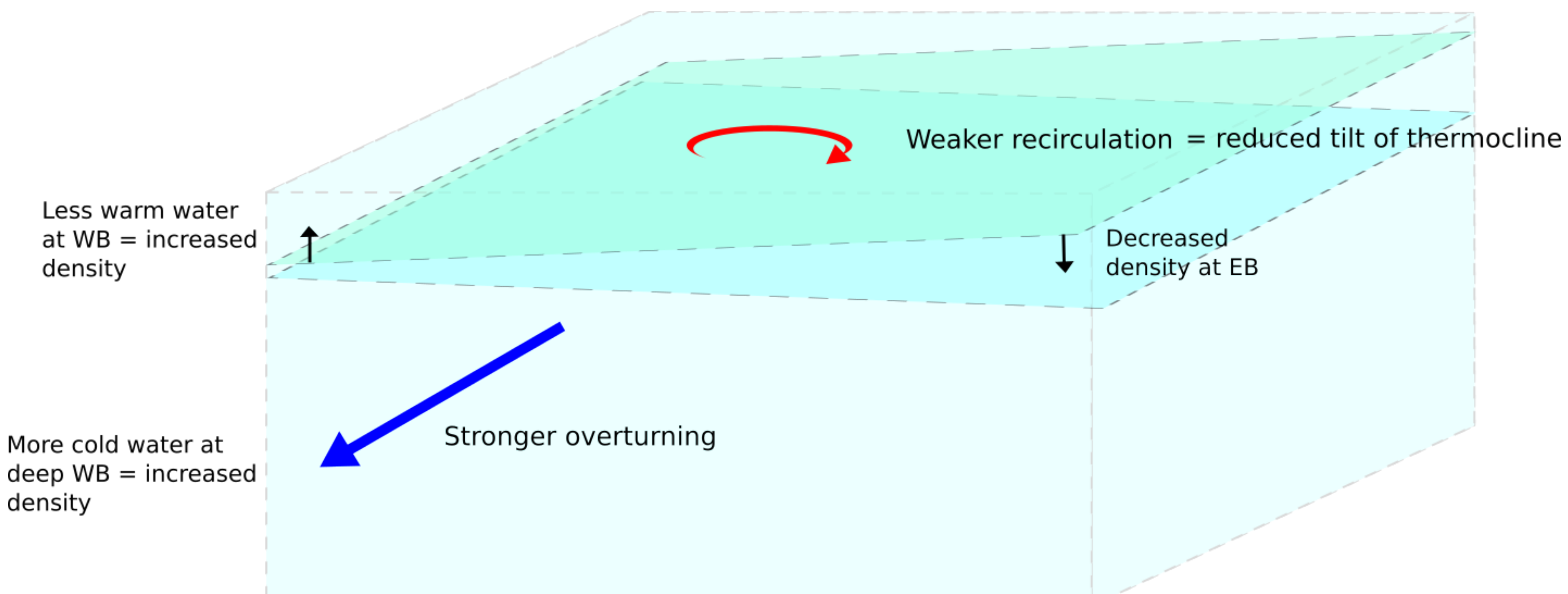

Weaker southwards recirculation in upper layer

Stronger deep return flow

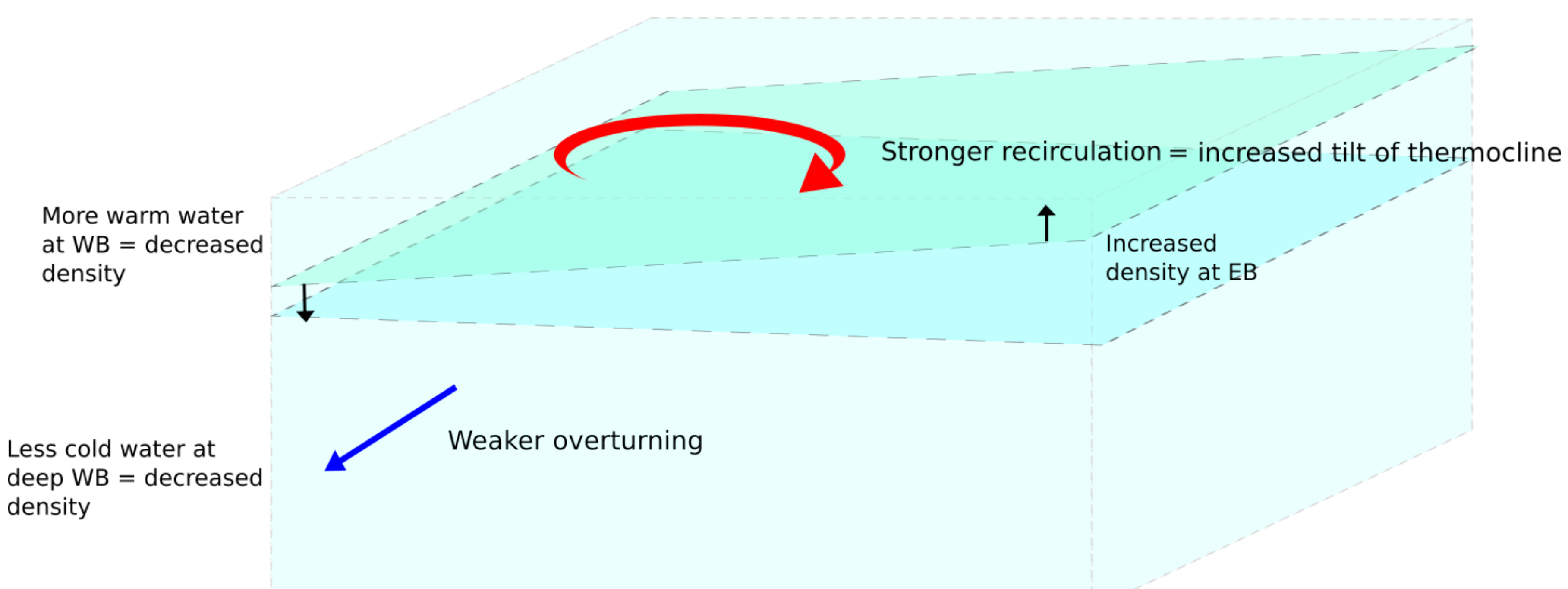

Stronger southwards recirculation in upper layer

Weaker deep return flow

Multiple linear regression models

Selecting explanatory variables

Strong correlation between isopycnal displacements and UMO transport on both western (solid) and eastern boundaries (dashed) above 1400 m

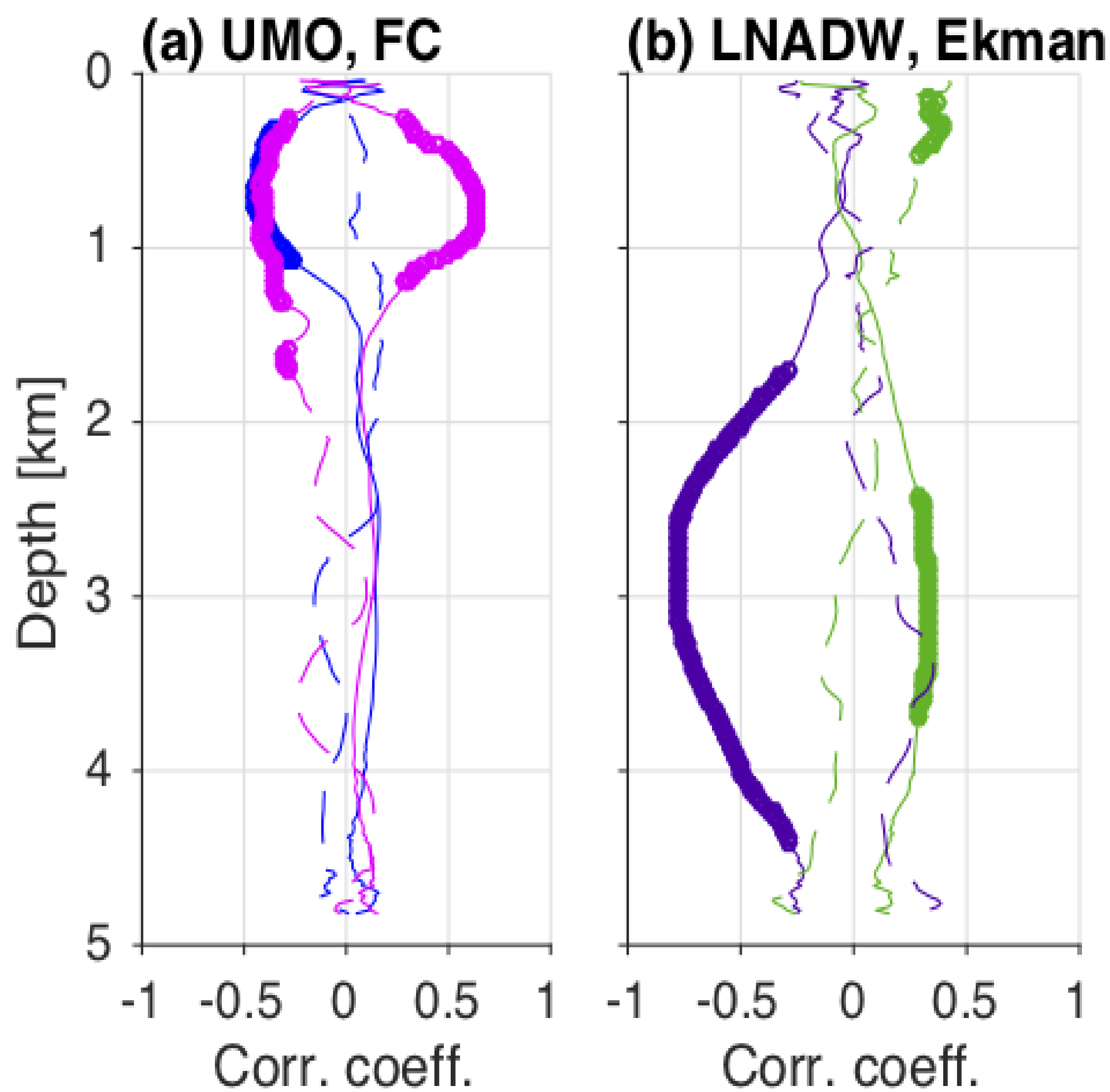

Strong correlation between deep western boundary density anomalies and LNADW transport

Fig. 8, Frajka-Williams et al., (2016)

Selecting explanatory variables

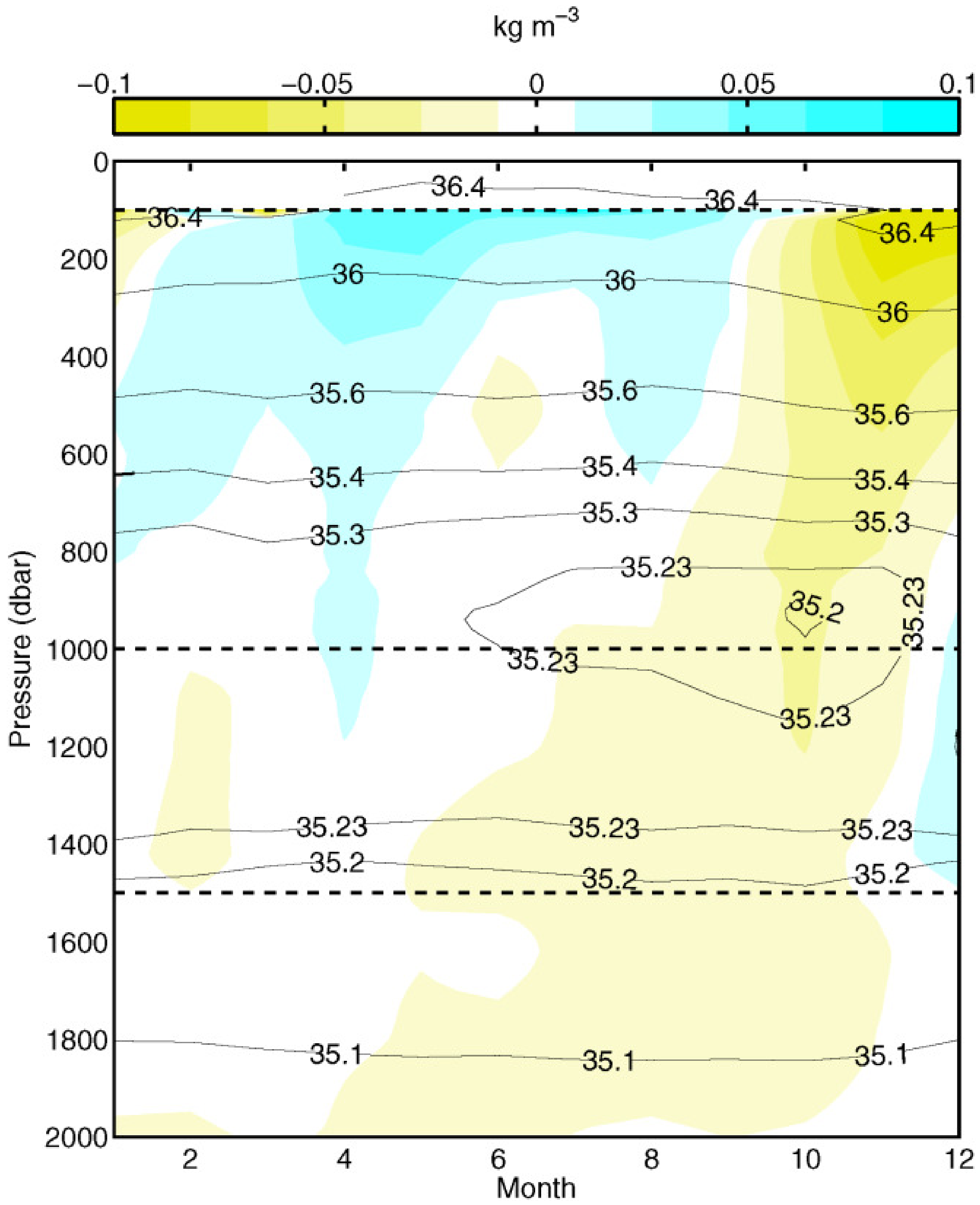

Fig. 11, Péréz-Hernández et al., (2015)

UMO seasonality is driven by eastern boundary density anomalies centered around 1000 m

Chidichimo et al., (2010), Péréz-Hernández et al., (2015) TODO - 3/4 layer model schematic, showing relationship between layers and boundary density

Used an algorithm to find at which depths (p1, p2, p3, p4) the boundary density anomalies give the highest variance explained by the ordinary least-squares (OLS) multiple linear regression

$$UMO = \alpha \cdot \rho_{p1} + \beta \cdot \rho_{p2} + \gamma \cdot \rho_{p3} + \zeta \cdot \rho_{p4}$$

Model results

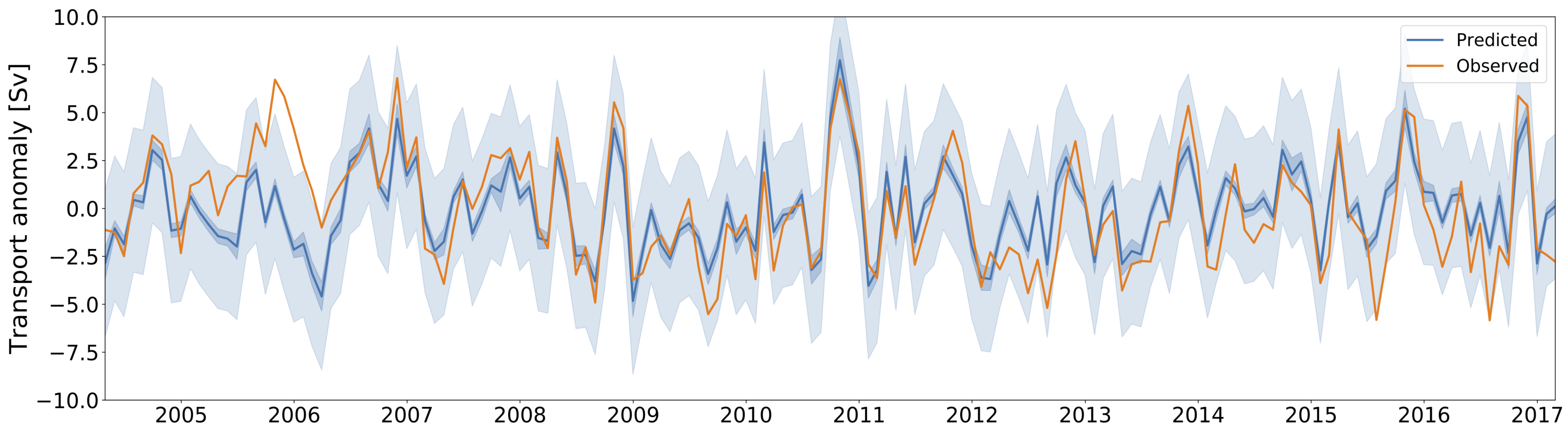

$$UMO = \alpha \cdot \rho_{wb}^{740} + \beta \cdot \rho_{eb}^{1020}$$

58% variance explained

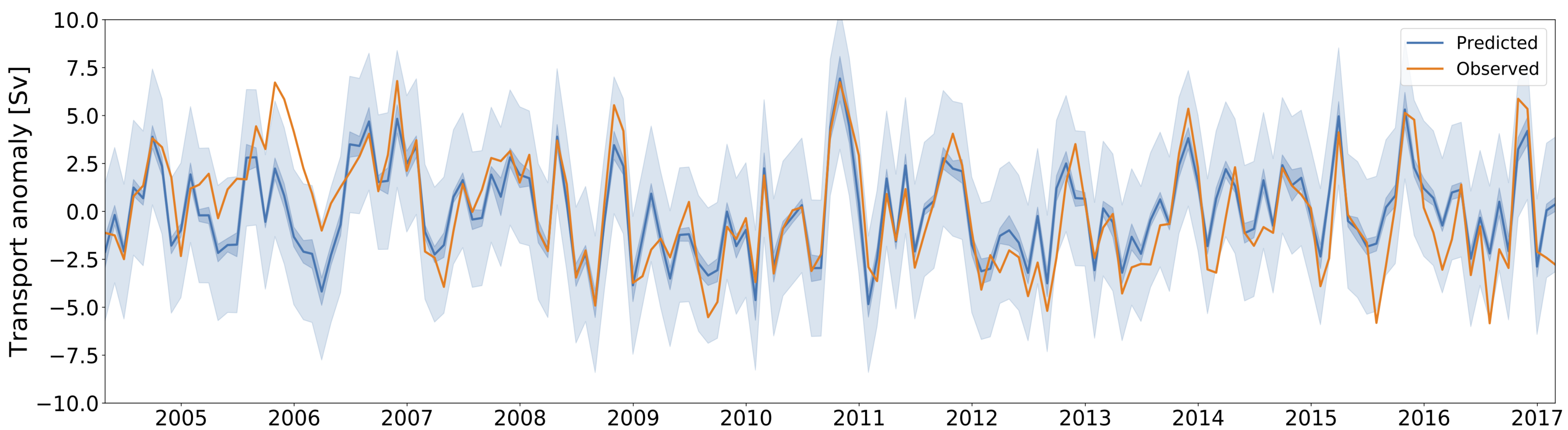

$$UMO = \alpha \cdot \rho_{wb}^{740} + \beta \cdot \rho_{eb}^{1020} + \gamma \cdot \rho_{wb}^{2840}$$

63% variance explained

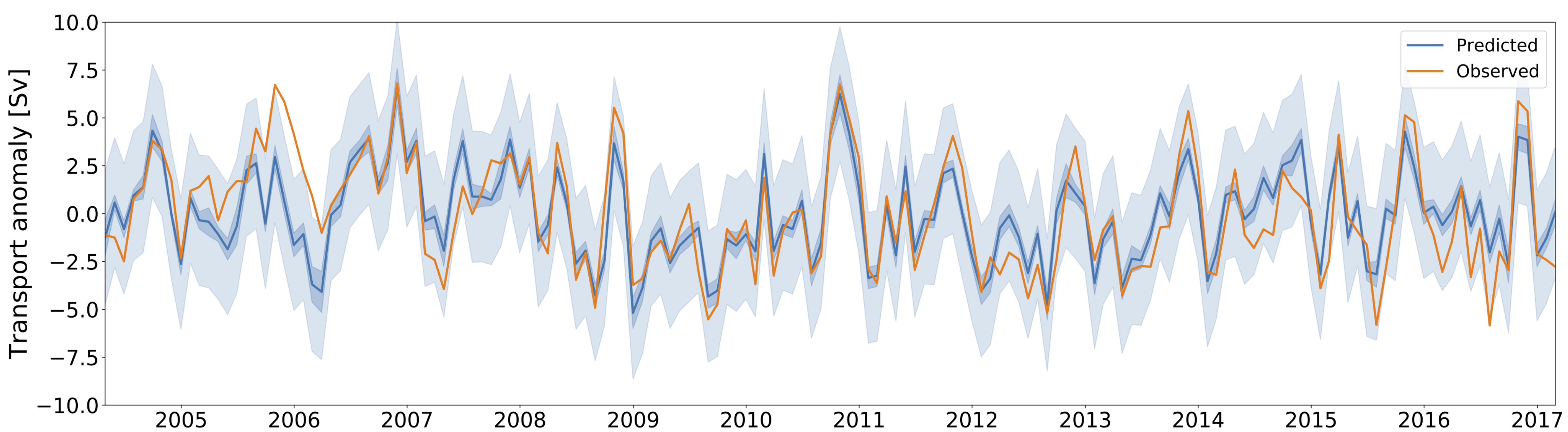

$$UMO = \alpha \cdot \rho_{wb}^{680} + \beta \cdot \rho_{eb}^{900} + \gamma \cdot \rho_{wb}^{1200} + \zeta \cdot \rho_{w}^{41}$$

70% variance explained

Assumptions of linear regression models

Four-variable OLS regression model failed 3 assumptions as it is based on a time series

- Autocorrelation of residuals
- Homoscedasticity (equal variance of residuals)
- Normal distribution of residuals

An alternative model is a generalized least-squares with autocorrelated errors (GLSAR)
McKinney et al., 2019

The significant partial autocorrelation gives the number of lags

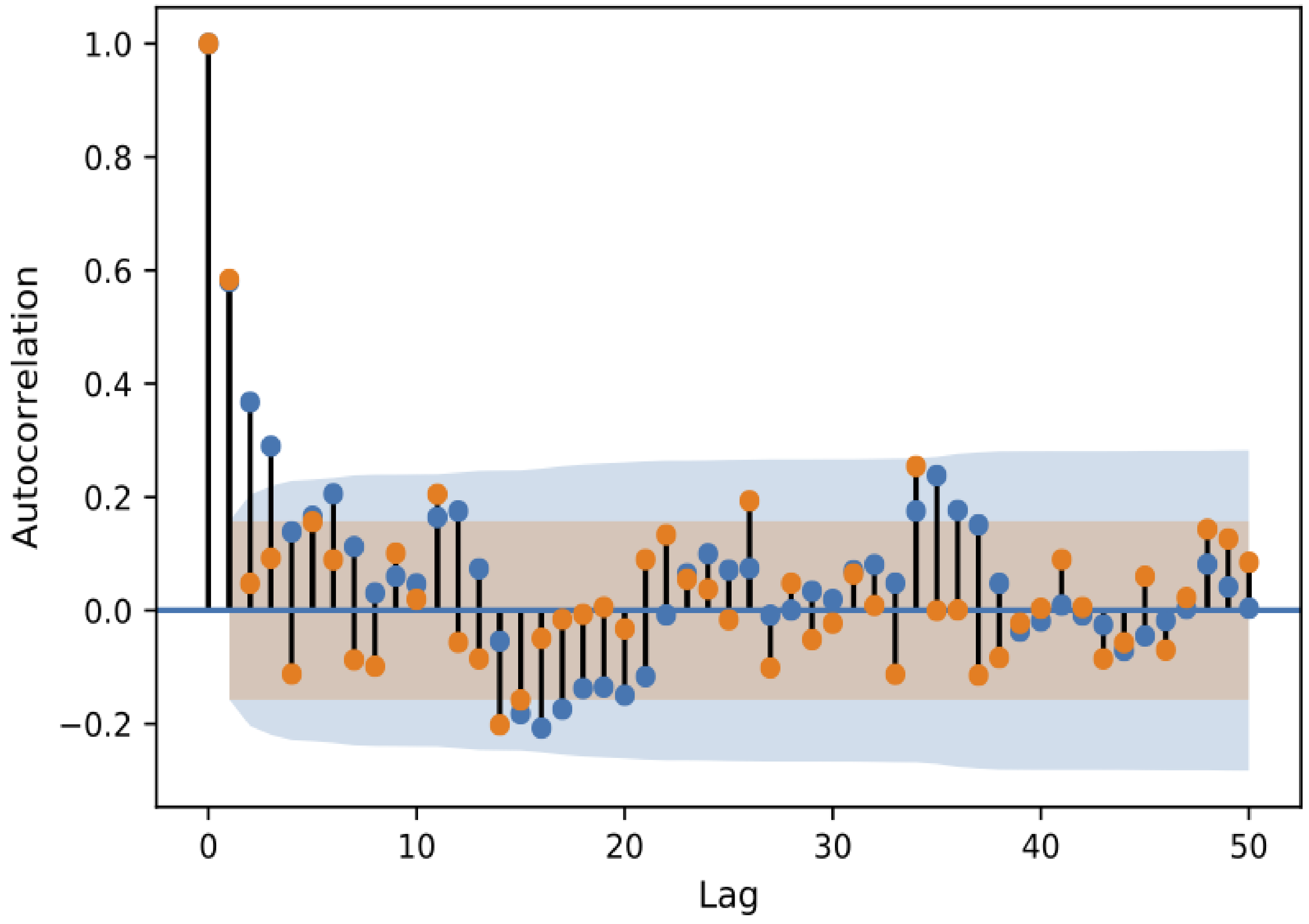

Autocorrelation and partial autocorrelation with 95% significance shaded

GLSAR(1) model

$$UMO = 38.04\,\rho_{720}^{wb} - 100.53\,\rho_{880}^{eb} + 54.83\,\rho_{1300}^{wb} + 129.05\,\rho_{4100}^{wb}$$

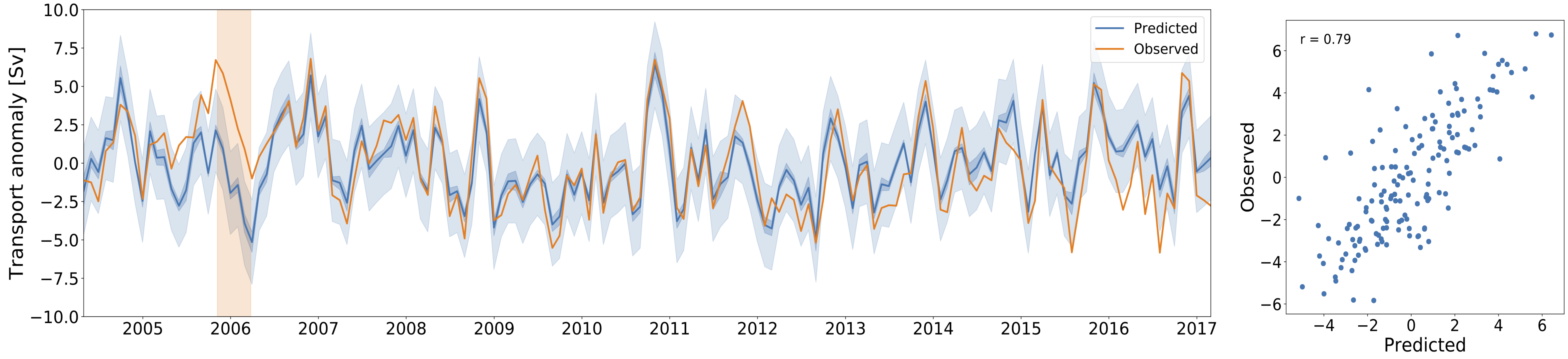

Observed monthly mean UMO transport compared to GLSAR(1) model results. Orange shaded area shows duration of WB" mooring collapse.

RMSE = 2.3 Sv

Cross-validation

Regression model created using first and last 60%, 70%, 80% and 90% of data

Model predicts UMO transport using remaining 40%, 30%, 20% and 10%

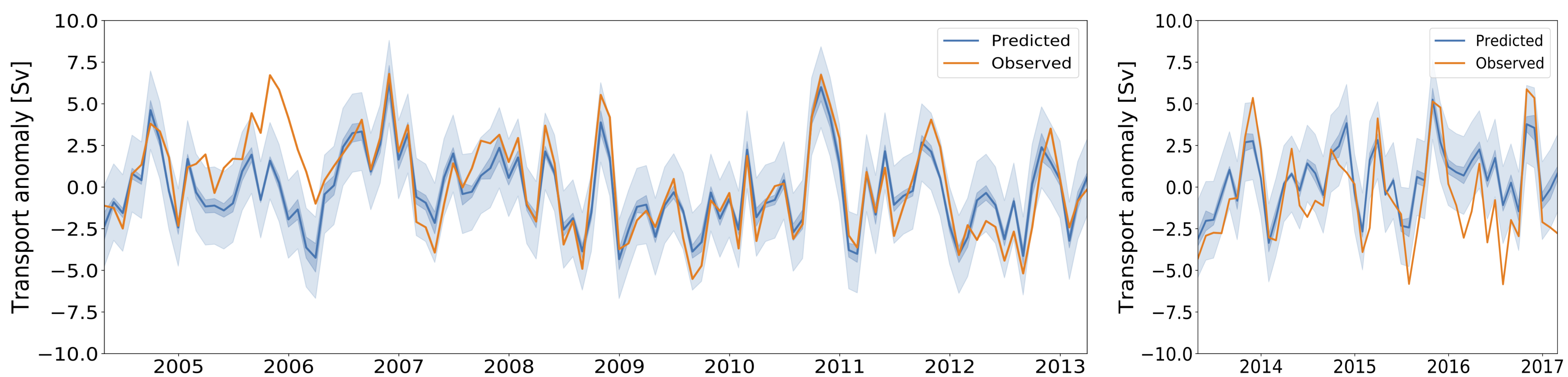

Model created with first 70% predicting last 30% - RMSE = 2.1 Sv

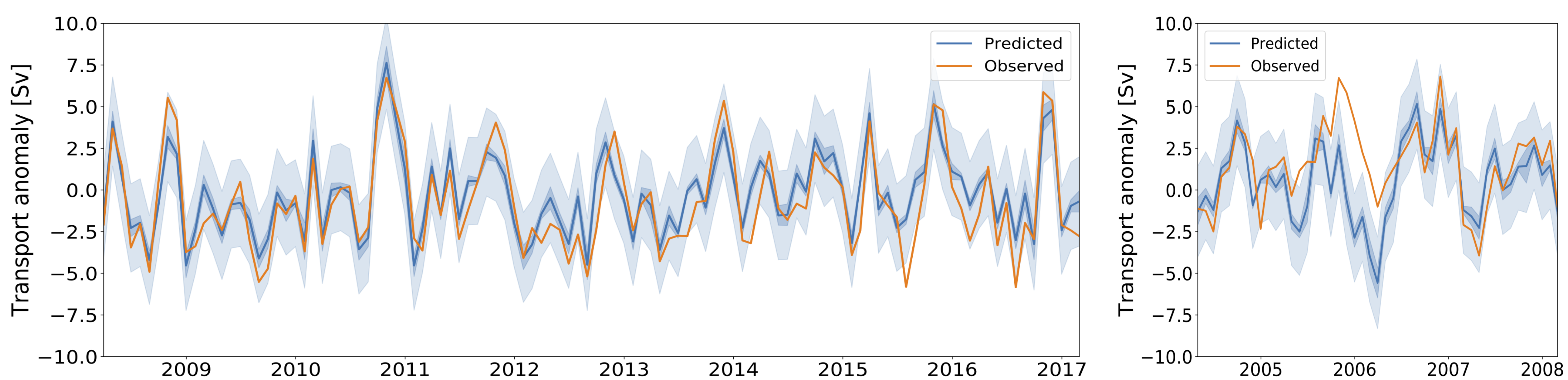

Model created with last 70% predicting first 30% - RMSE = 2.4 Sv

Cross-validation model results

	Min	Max
Explained variance	74%	81%
SE [Sv]	1.1	1.3

Cross-validation prediction results

	Min	Max
RMSE [Sv]	2.1	2.8
Percent in PI	58%	87%

Coherence between UMO and density anomalies

Thermocline [720 dbar]

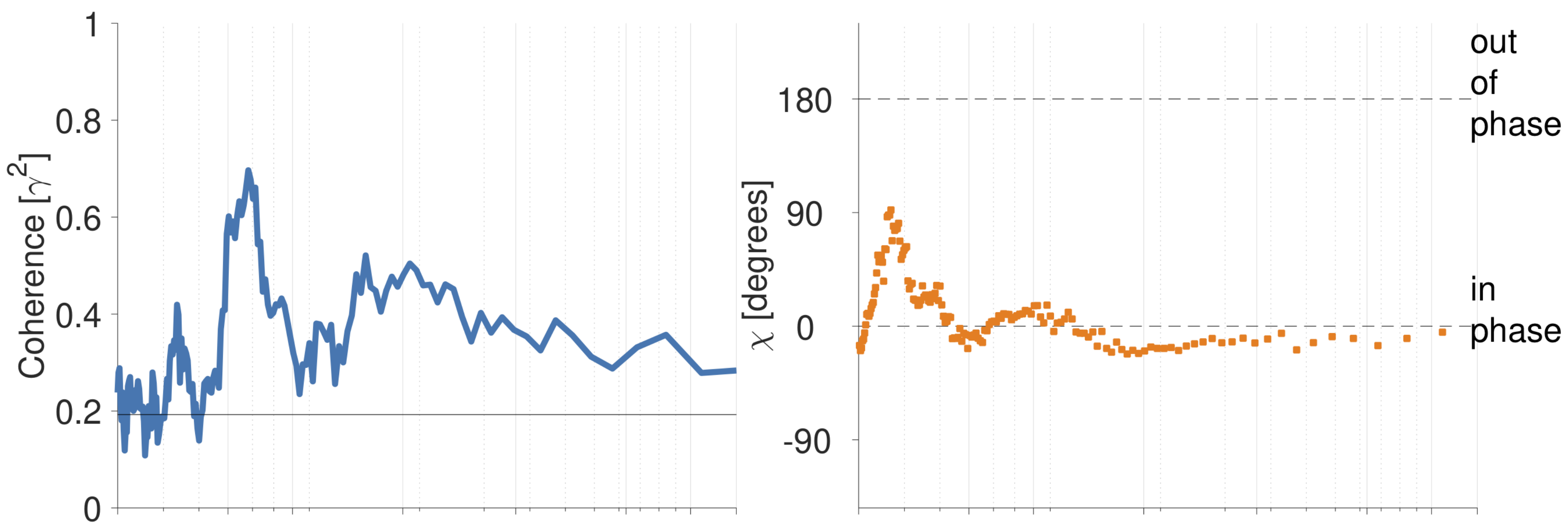

AAIW [880 dbar]

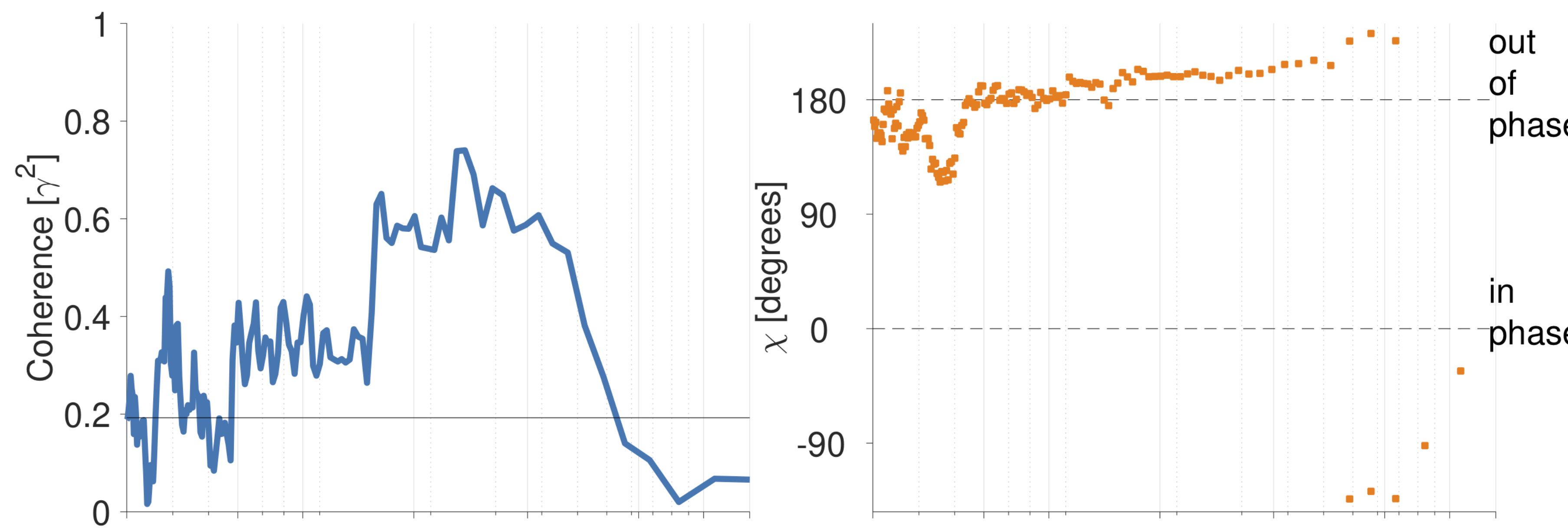

UNADW [1300 dbar]

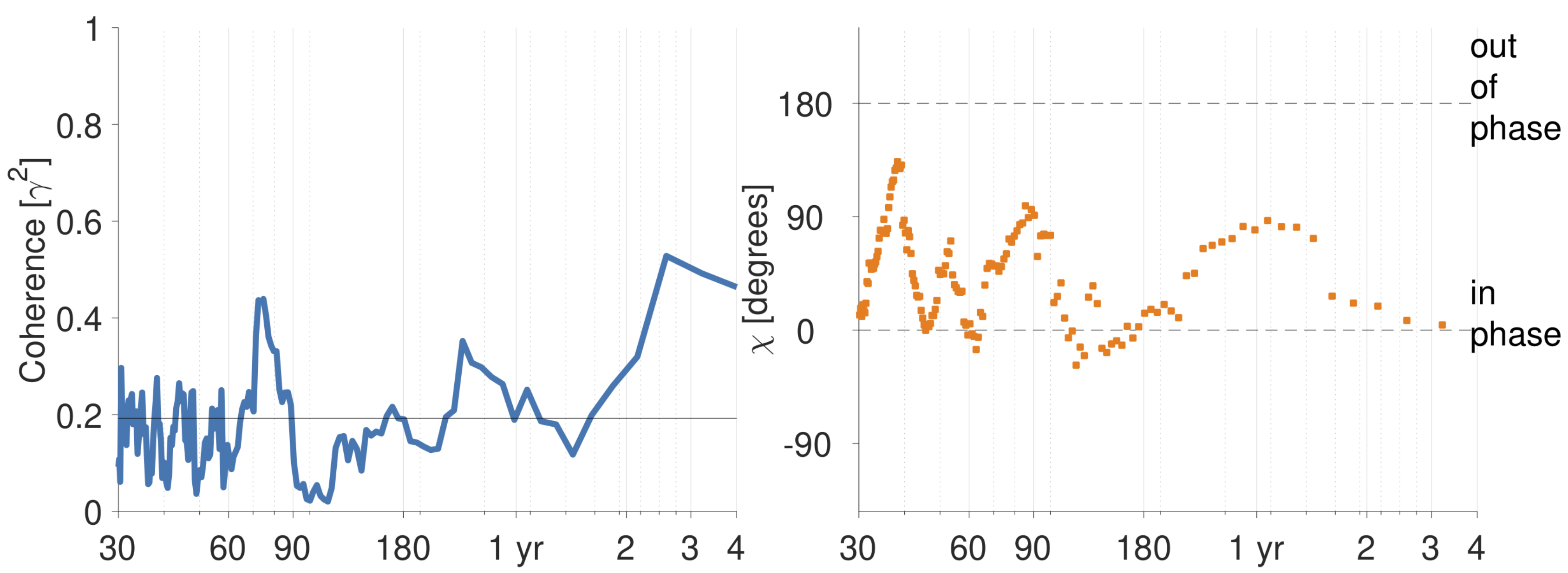

LNADW [4100 dbar]

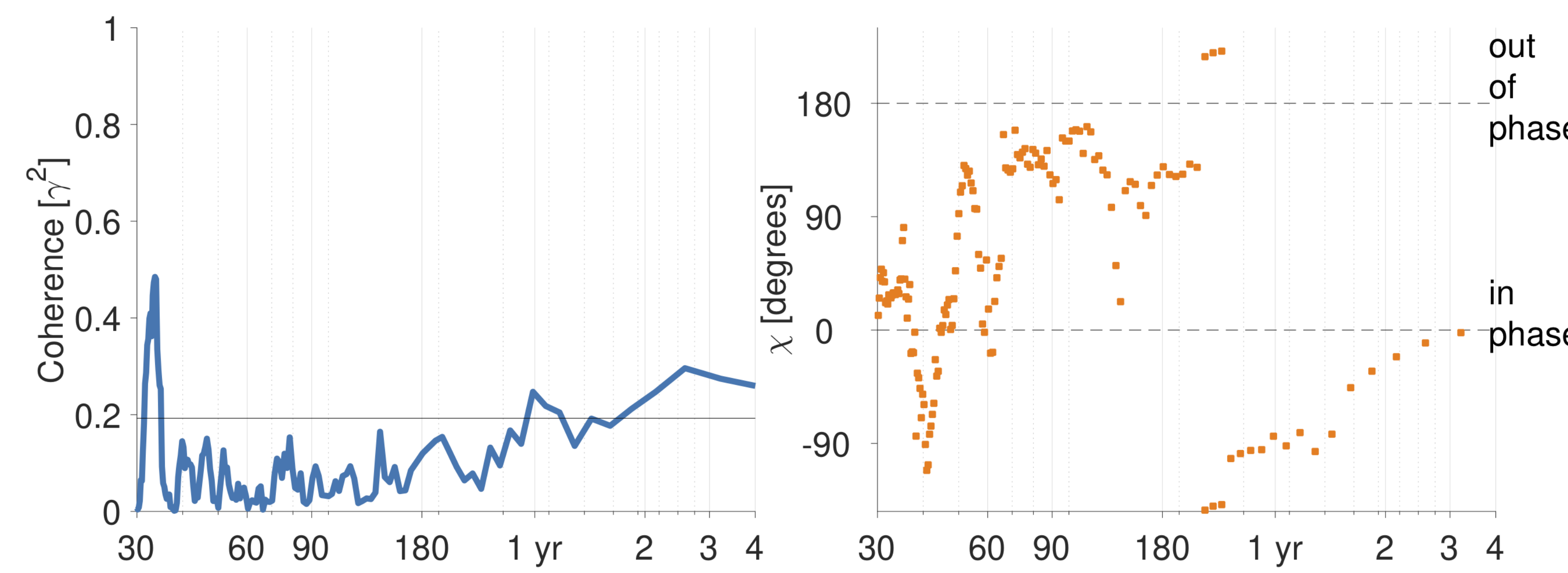

Conclusions

- At least 3 layers are required to explain more than 60% variance of UMO transport
- GLSAR model using 4 boundary density anomalies explains 73% of the variance in the observed transport
- Cross-validation shows a maximum root-mean-square error of 2.8 Sv and mean of 2.3 Sv
- Regression model captures variability on all timescales:
  - Seasonal variability dominated by AAIW layer
  - Longer timescale variability found in thermocline and deeper layers

Future work

- Test model against new RAPID results and hydrographic section data - is level of uncertainty reasonable?
- Assess whether seasonal climatology can replace eastern boundary variable
- Apply model to historical CTD and mooring data
- Investigate model further using NEMO ocean model with 1/12° resolution

References

Bryden, H. L., Longworth, H. R., & Cunningham, S. A. (2005). Slowing of the Atlantic meridional overturning circulation at 25°N. Nature, 438(7068), 655–657.

Chidichimo, M. P., Kanzow, T., Cunningham, S. A., Johns, W. E., & Marotzke, J. (2010). The contribution of eastern-boundary density variations to the Atlantic meridional overturning circulation at 26.5°N. Ocean Science, 6(2), 475–490.

Frajka-Williams, E., Meinen, C. S., Johns, W. E., Smeed, D. A., Duchez, A., Lawrence, A. J., … Rayner, D. (2016). Compensation between meridional flow components of the Atlantic MOC at 26°N. Ocean Science, 12(2), 481–493.

Longworth, H. R., Bryden, H. L. and Baringer, M. O. (2011) Historical variability in Atlantic meridional baroclinic transport at 26.5°N from boundary dynamic height observations, Deep-Sea Research Part II (58), 1754–1767.

McKinney, W., Perktold, J., & Seabold, S. (2019). Time Series Analysis in Python with statsmodels.

Pérez-Hernández, M. D., McCarthy, G. D., Vélez-Belchí, P., Smeed, D. A., Fraile-Nuez, E., & Hernández-Guerra, A. (2015). The Canary Basin contribution to the seasonal cycle of the Atlantic Meridional Overturning Circulation at 26°N. Journal of Geophysical Research: Oceans, 120(11), 7237–7252.

Thank you

Any questions?